

Computational Modeling of the Dehydrogenation of Methylamine

Kirsten Ivey, Belynda Sanders, Chris Estela, and Andrew L. Cooksy*

Department of Chemistry and Biochemistry; San Diego State University; San Diego, CA 92182-1030.

*corresponding author; Department of Chemistry and Biochemistry; San Diego State University; San Diego, CA 92182-1030;

e-mail: acooksy@sciences.sdsu.edu; tel: +1-619-594-5571.

Received June 14, 2010; accepted October 12, 2010

Abstract. The reaction sequence early in the metabolism of methylamine by the dehydrogenase cofactor tryptophan tryptophyl quinone (TTQ) is investigated by a large series of density functional theory calculations. Free energy corrections are calculated at the reactant and intermediate geometries, and solvation effects are estimated by use of the semi-empirical COSMO-RS solvent model. Two competing reaction paths are found to have very similar reaction free energies, and the free energies of activation are found to depend heavily on adequate modeling of the solvent.

Keywords: Tryptophan tryptophyl quinone; TTQ; density functional theory; COSMO-RS; solvent model.

Introduction

The metabolism of methylamine by methylamine dehydrogenase (MAD) in anaerobic bacteria, $\text{H}_2\text{O} + \text{CH}_3\text{NH}_2 \xrightarrow{\text{MAD}} \text{H}_2\text{CO} + \text{NH}_3 + 2\text{H}^+$ offers a relatively simple stage for investigations of fundamental biochemical processes involving proton and electron transfer. The reactive site of the MAD is the cofactor tryptophan tryptophyl quinone (TTQ, Figure 1), which metabolizes methylamine by reaction with water over several steps.

The reactions of TTQ have been extensively characterized in experimental work by Davidson and others, beginning in the 1990s [1-4]. More recent work includes computationally-assisted assignment of the IR spectrum of TTQ in the enzyme complex [5] and a high-level computational analysis of the effects of tunneling on one subset of the reactions [6]. It has generally been assumed that reaction is initiated by attachment of methylamine to the carbonyl beta to the pyrrole ring (reaction path **a**), although in principle reaction could occur at the second carbonyl as well (reaction path “**b**”). In this paper, we

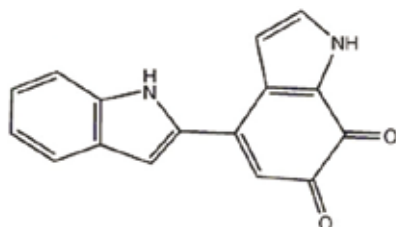


Fig. 1. The TTQ cofactor.

Resumen. Se investigaron las reacciones tempranas en el metabolismo de la metilamina por el cofactor quinon-triptofil-triptofano (TTQ), mediante una larga serie de cálculos de la teoría de funcionales de la densidad. Las correcciones a las energías libres se calcularon en las geometrías del reactivo y de los intermediarios, así como los efectos del disolvente se estimaron por el modelo semi-empírico COSMO-RS. Se encontró que dos caminos de reacción compiten, teniendo energías libres de reacción muy similares, y las energías libres de activación dependen mucho de un modelado adecuado del disolvente.

Palabras clave: quinon-triptofil-triptofano; TTQ; teoría de funcionales de la densidad; COSMO-RS; modelo del disolvente.

present calculations on the first several steps of the metabolism of methylamine, employing a realistic solvent correction and testing the viability of both the **a** and **b** reaction pathways.

Results and Discussion

Five elementary reaction steps were modeled for each of the **a** and **b** reaction pathways. The steps for the **a** pathway are shown in Figure 2. This reaction sequence completes the hydrogen shifts that need to take place just prior to the liberation of formaldehyde. The optimized geometries for intermediates **2a** and **2b**, formed by attachment of methylamine to TTQ, are shown in Figure 3. The remaining structures in reaction path **a** are shown in Figure 4.

The calculated free energies of reaction for each step of the **a** and **b** reaction mechanisms are given in Table 1. We note that the attachment of the methylamine, although exothermic in the gas phase ($\Delta E_{\text{gas}} < 0$ in Table 1), is prevented from being spontaneous when free energy corrections are applied ($\Delta G > 0$ in Table 1). The gas-phase energies of reaction ΔE themselves are virtually meaningless in ion-mediated reactions if no solvent correction is applied, as seen by the wide range of values encountered in Table 1. This is frequently encountered in computational models of solvent-phase association reactions. However, by probing the reaction coordinates directly, we are able to observe, for example in the reaction of **2a** to **3a**, a slight barrier to dissociation. The resulting complex **2** then reacts rapidly and vigorously to dispose of the dangling OH group, yielding the iminium ion **3**.

The third step of the reaction, deprotonation of the methyl group to form **4** from **3**, presents a substantial barrier and is substantially endergonic ($\Delta G > 0$). Again, the reaction is as-

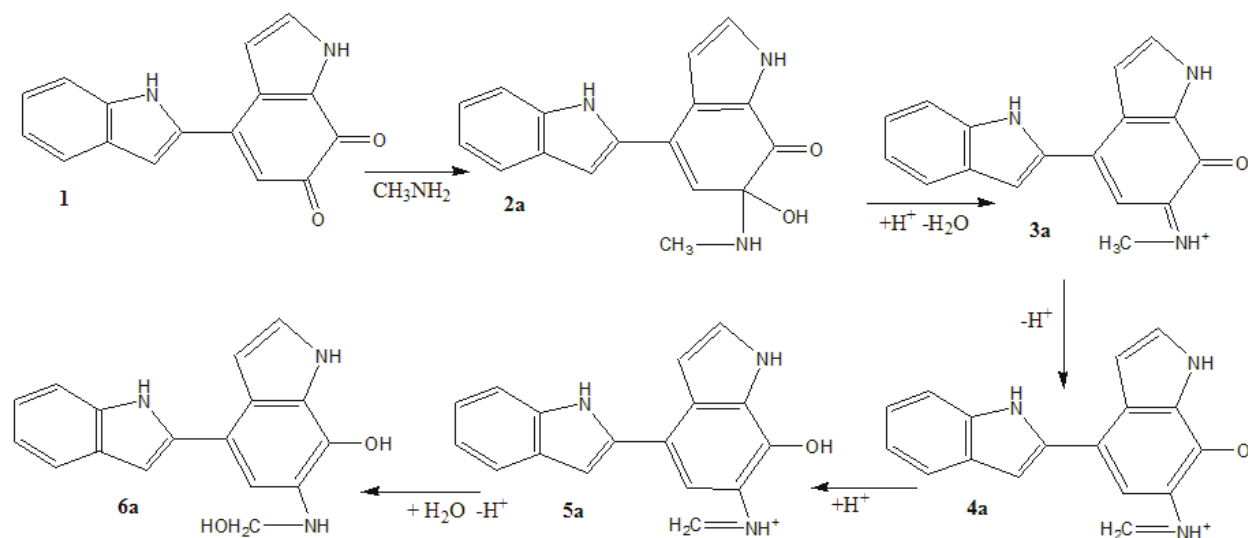


Fig. 2. Proposed reaction scheme a for partial metabolism of methylamine to formaldehyde.

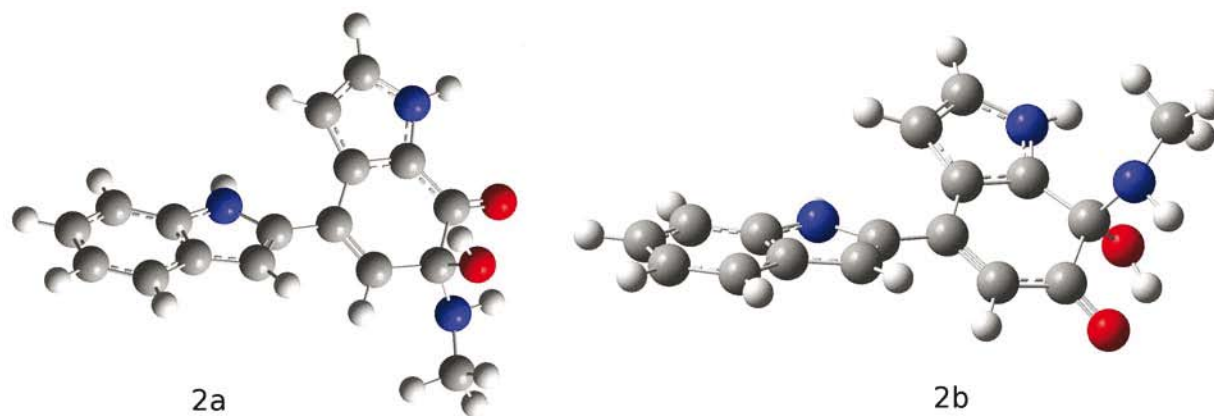


Fig. 3. B3LYP/cc-pVDZ optimized geometries of intermediates 2a and 2b.

sisted by a very fast follow-up reaction, in this case protonation of the alkoxy anion to yield **5**. The final step in the sequence, hydration of the methylene group, is also endergonic, by virtue of removing one water molecule from solution.

The individual reaction steps and the net reaction are all predicted to be quite similar energetically whether following reaction path **a** or path **b**, with **b** being slightly more favored. Although individual steps offer significant barriers, these are substantially ameliorated by the solvent stabilization of charge

carriers, and the net reaction to form **6** from **1** has a ΔG of only a few kcal/mol. The overall reaction is driven by the subsequent dissociation of formaldehyde.

The kinetics of the reaction are unfortunately much more difficult to assess. Because the potential energy surface for the reaction cannot be searched in conjunction with the COSMO-RS correction, geometries and energies of the transition states can only be estimated. For each step, we carried out partial optimizations of the reaction system, fixing a key bond distance

Table 1. Free energies of reaction for pathways **a** and **b** and estimated free energies of activation (without vibrational corrections) for path **a**.

Reactant	Product	$\Delta E_{\text{gas}}(\text{a})$ (kcal/mol)	$\Delta G(\text{a})$ (kcal/mol)	$\Delta E_{\text{gas}}(\text{b})$ (kcal/mol)	$\Delta G(\text{b})$ (kcal/mol)	Approx $G_{\text{a}}(\text{a})$ (kcal/mol)
1 + CH_3NH_2	2	-3.7	17.8	-6.0	18.8	21
2 + H_3O^+	3 + 2 H_2O	-82.2	-40.0	-71.6	-37.4	3
3 + H_2O	4 + H_3O^+	0.2	16.8	8.3	16.9	28
4 + H_3O^+	5 + H_2O	-64.4	-12.2	-66.2	-13.2	6
5 + 2 H_2O	6 + H_3O^+	-17.1	25.0	-15.4	20.3	39

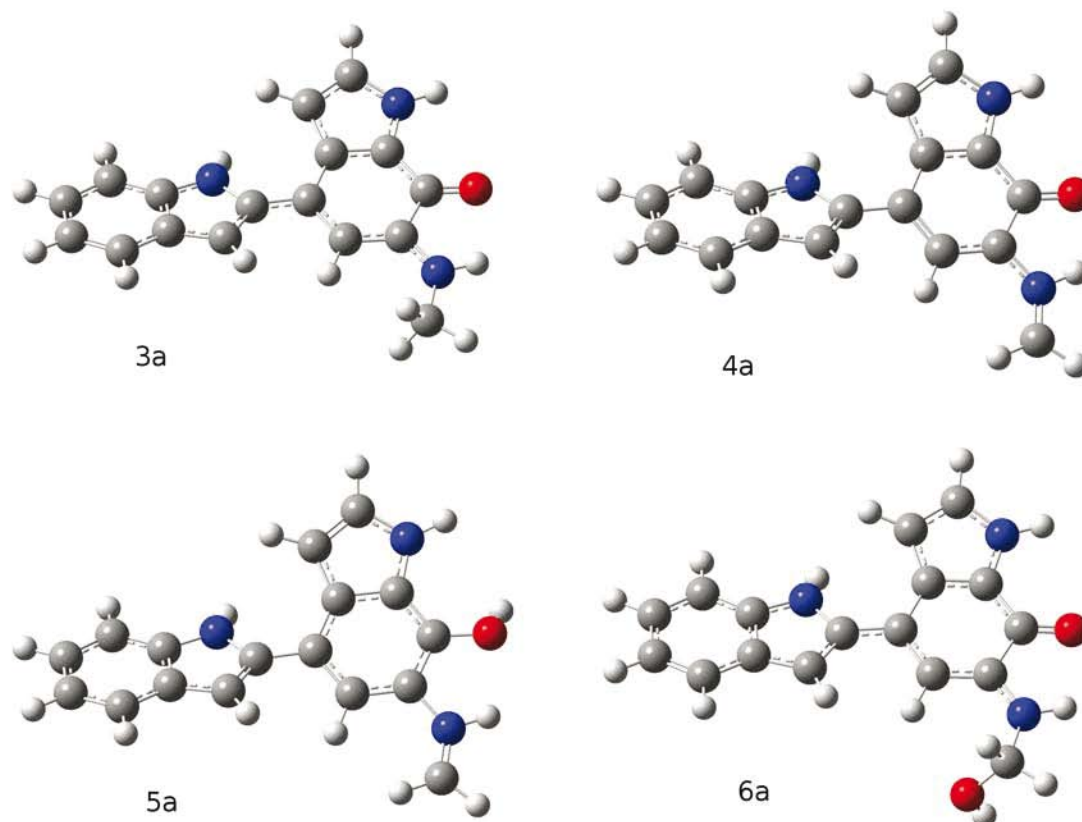


Fig. 4. B3LYP/cc-pVDZ optimized geometries of species 3a-6a.

for the reaction. This allows the calculation of a gas-phase reaction diagram, such as the one shown in Figure 5. At each of these geometries, we can then calculate the solvent correction using first the COSMO PCM method, which provides the input for the COSMO-RS calculation. However, this allows us

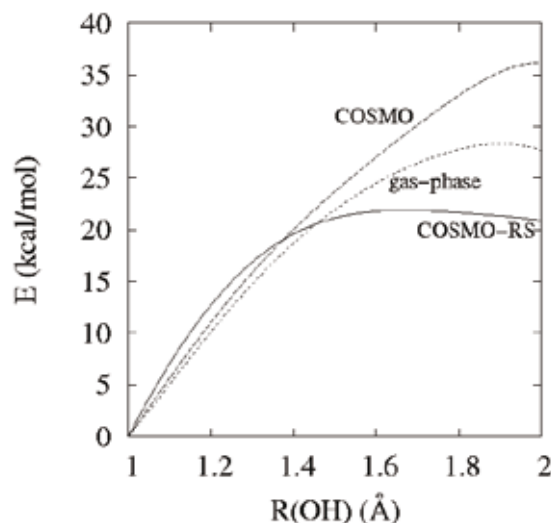


Fig. 5. Comparison of step 2a ($2a + \text{H}_3\text{O}^+ \rightarrow 3a + 2\text{H}_2\text{O}$) reaction diagrams for different approximations.

to find only an upper limit to the activation barrier, because we cannot optimize the molecular geometries at the same time the COSMO-RS solvent correction is applied. Furthermore, because these geometries in the middle of the reaction diagram are not stationary points on the potential energy surface, standard means for estimating the vibrational energies are invalid. The values given in Table 1 for the approximate activation free energies therefore reflect free energy contributions from the solute-solvent interaction, but do not include the vibrational corrections for free energy. Approximate transition state structures are shown in Figure 6.

As an example, crude reaction diagrams for the conversion of 2 to 3 are drawn in Figure 5. Using the O-H^+ separation as a reaction coordinate, the forward reaction proceeds from right to left in Figure 5 (as the H^+ approaches and scavenges the OH to form water and transfer charge to the TTQ). Energies are shown for the B3LYP/cc-pVDZ uncorrected energies (“gas-phase”), the BP86/TZVP COSMO-corrected free energies, and the COSMO-RS corrected free energies. The geometries in the graph are not stationary points for the most part, and the energies do not include vibrational corrections. However, it is still seen that overall the reaction step is exothermic, consistent with the large negative ΔG in Table 1. Figure 5 illustrates a common feature of these reaction diagrams: gas-phase models and PCM solvent models tend to greatly underestimate the stability

of small molecular ions, in this case, the H_3O^+ used to provide the proton. As a result, computational models of the reaction kinetics can be problematic, with barriers often absent in the gas-phase and PCM calculations. In this case, the COSMO-RS model predicts sufficient stabilization of the ion that a small barrier to the reaction appears.

All B3LYP and BP86 calculations were carried out using *Gaussian 03* [7] on various Linux platforms. The COSMO-RS calculations were computed using *COSMOtherm* [8].

Conclusions

We have found that two reaction pathways for the metabolism of methylamine by TTQ occur along similar free energy contours, weakly favoring methylamine attachment at the carbonyl

group furthest from the pyrrole heterocycle. Furthermore, we find that accurate solvent modeling may be essential to the adequate prediction of reaction properties for this system by DFT calculations. No direct experimental measurements have been made on these reaction intermediates to date, and only global kinetics data are available. Continuing work in our laboratory will assess the free energies of activation more precisely and extend the work to complete the conversion of methylamine to formaldehyde and ammonia, allowing for direct comparison to laboratory data.

Methods

Geometry optimizations and frequency calculations were carried out using the B3LYP hybrid density functional method and

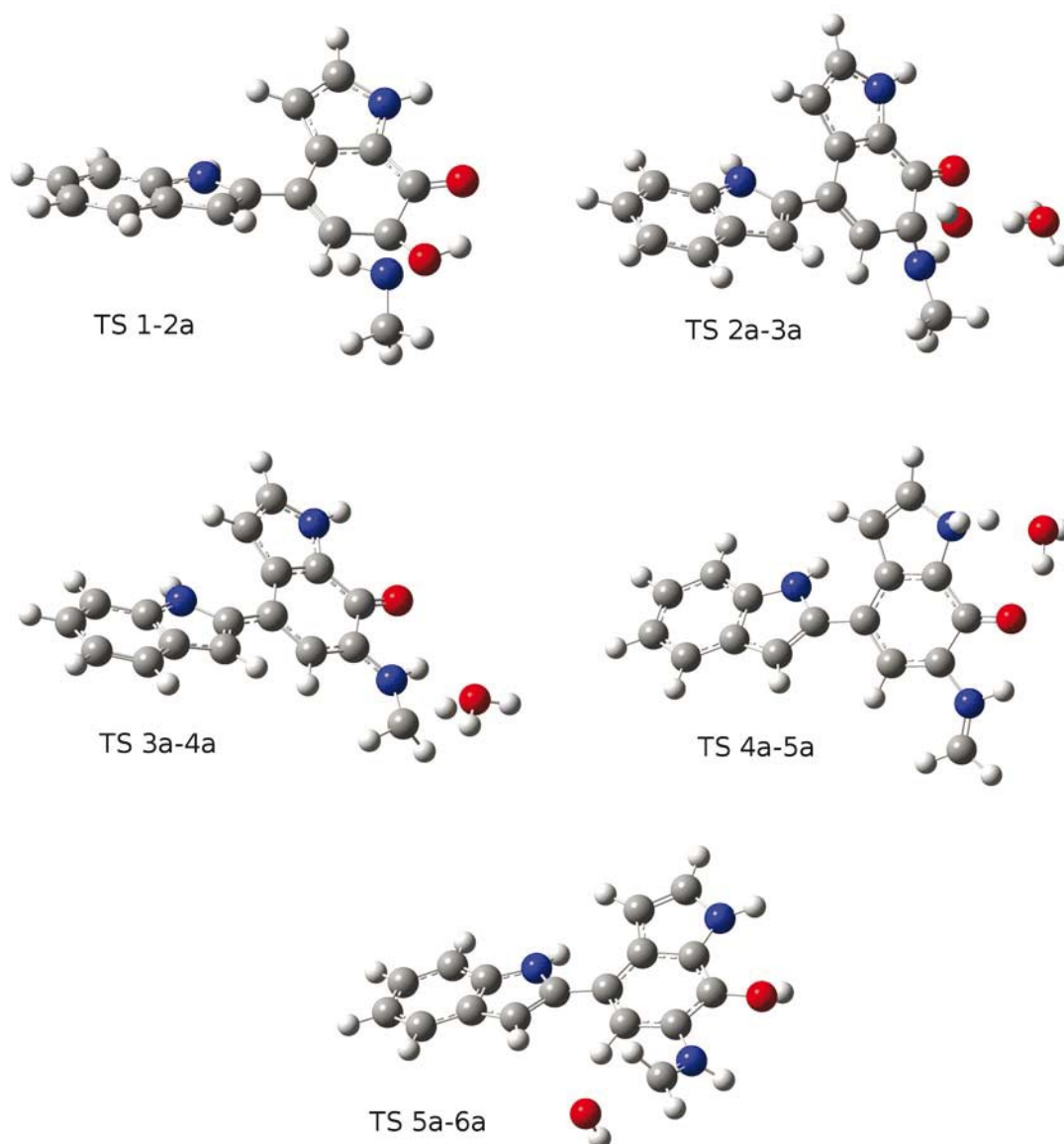


Fig. 6. B3LYP/cc-pVDZ optimized geometries near solvent-corrected activation barriers.

Dunning's cc-pVDZ basis set [9-11]. Although these methods appear to be accurate to within roughly 2 kcal/mol for small molecules in the gas phase, the ionic components of some of the reactions in the current system are strongly stabilized by the surrounding solvent. These stabilization energies in aqueous media cannot be adequately modeled by standard polarizable continuum methods (PCMs). In our previous study of reactions involving tocopherol [12], we found that the COSMO-RS method was capable of far more accurate solvent modeling [13]. Therefore, at each optimized geometry in the present work, a COSMO PCM calculation was carried out at the BP86/TZVP/DGA1 level [14-17] in order to evaluate the triple-zeta-quality COSMO-RS solvent correction. Frequency calculations were carried out for each of the optimized geometries to compute the zero-point and thermal energy contributions to the molecular free energies. The final quoted free energies are based on BP86/TZVP electronic and solvation energies at the B3LYP/cc-pVDZ optimized geometries, with B3LYP/cc-pVDZ vibrational corrections.

For each step of the reaction, we also freeze the coordinates of the interacting atoms at various increments of 0.2 Å and optimize the intermediate geometries at each increment, in order to assemble a crude reaction diagram, and estimate the free energy of activation. Many of the reaction paths show no evidence of a reaction barrier in the gas-phase energies, requiring solvent corrections to adequately model the solvent stabilization at both ends of the reaction. As a result, it is not possible to analytically optimize the transition states. For the present, free energies of activation were estimated from the coarse reaction diagrams, and the resulting error is estimated to be 2 kcal/mol.

Acknowledgements

This work was originally supported by the Blasker Fund of the San Diego Foundation. Computer resources have been provided under US National Science Foundation Grant CHE-0216563. B. Sanders, C. Estela, and K. Ivey were supported by NIW fellowships from the US National Institutes of Health.

References

1. Backes, G.; Davidson, V. L.; Huitema, F.; Duine, J. A.; Sanders-Loehr, J. *Biochemistry* **1991**, *30*, 9201-9210.
2. Davidson, V. L.; Kumar, M. A.; Wu, J. *Biochemistry* **1992**, *31*, 1504-1508.
3. McIntire, W. S. *FASEB J.* **1994**, *8*, 513-21.
4. Klinman, J. P.; Mu, D. *Ann. Rev. Biochem.* **1994**, *63*, 299-344.
5. Pang, J.; Scrutton, N. S.; de Visser, S. P.; Sutcliffe, M. J. *J. Phys. Chem. A* **2010**, *114*, 1212-1217.
6. Masgrau, L.; Ranaghan, K. E.; Scrutton, N. S.; Mulholland, A. J.; Sutcliffe, M. J. *J. Phys. Chem. B* **2007**, *111*, 3032-3047.
7. Frisch, M. J.; Trucks, G. W.; Schlegel, H. B.; Scuseria, G. E.; Robb, M. A.; Cheeseman, J. R.; Montgomery, Jr., J. A.; Vreven, T.; Kudin, K. N.; Burant, J. C.; Millam, J. M.; Iyengar, S. S.; Tomasi, J.; Barone, V.; Mennucci, B.; Cossi, M.; Scalmani, G.; Rega, N.; Petersson, G. A.; Nakatsuji, H.; Hada, M.; Ehara, M.; Toyota, K.; Fukuda, R.; Hasegawa, J.; Ishida, M.; Nakajima, T.; Honda, Y.; Kitao, O.; Nakai, H.; Klene, M.; Li, X.; Knox, J. E.; Hratchian, H. P.; Cross, J. B.; Adamo, C.; Jaramillo, J.; Gomperts, R.; Stratmann, R. E.; Yazyev, O.; Austin, A. J.; Cammi, R.; Pomelli, C.; Ochterski, J. W.; Ayala, P. Y.; Morokuma, K.; Voth, G. A.; Salvador, P.; Dannenberg, J. J.; Zakrzewski, V. G.; Dapprich, S.; Daniels, A. D.; Strain, M. C.; Farkas, O.; Malick, D. K.; Rabuck, A. D.; Raghavachari, K.; Foresman, J. B.; Ortiz, J. V.; Cui, Q.; Baboul, A. G.; Clifford, S.; Cioslowski, J.; Stefanov, B. B.; Liu, G.; Liashenko, A.; Piskorz, P.; Komaromi, I.; Martin, R. L.; Fox, D. J.; Keith, T.; Al-Laham, M. A.; Peng, C. Y.; Nanayakkara, A.; Challacombe, M.; Gill, P. M. W.; Johnson, B.; Chen, W.; Wong, M. W.; Gonzalez, C.; Pople, J. A.; *Gaussian 03*, Revision B.02, Gaussian, Inc., Pittsburgh PA, 2003.
8. Eckert, F.; Klamt, A. *AiCHE J.* **2002**, *48*, 369-385.
9. Becke, A. D. *J. Chem. Phys.* **1993**, *98*, 5648-5652.
10. Lee, C.; Yang, W.; Parr, R. G. *Phys. Rev. B* **1988**, *37*, 785-789.
11. Dunning, J. T. H. *J. Chem. Phys.* **1989**, *90*, 1007-1023.
12. Lui, R.; Cooksy, A. L. *J. Comp. Theor. Chem.* **2006**, *2*, 1395-1402.
13. Klamt, A. *J. Phys. Chem.* **1995**, *99*, 2224-2235.
14. Becke, A. D. *Phys. Rev. A*, **1988**, *38*, 3098-100.
15. Perdew, J. P. *Phys. Rev. B*, **1986**, *33*, 8822-8824.
16. Schafer, A.; Huber, C.; Ahlrichs, R. *J. Chem. Phys.*, **1994**, *100*, 5829-5835.
17. Godbout, N.; Salahub, D. R.; Andzelm, J.; Wimmer, E. *Can. J. Chem.* **1992**, *70*, 560-571.